

The role and mechanism of the annexin A1 peptide Ac2-26 in rats with cardiopulmonary bypass lung injury

Jiyang Xu^{1,2}  | Chengkun Yu² | Junli Luo¹ | Yuhan Guo^{1,2} | Chi Cheng² | Hong Zhang¹ 

¹Department of Anesthesiology, Affiliated Hospital of Zunyi Medical University, Zunyi, China

²Guizhou Key Laboratory of Anesthesia and Organ Protection, Zunyi Medical University, Zunyi, China

Correspondence

Hong Zhang, Department of Anesthesiology, Affiliated Hospital of Zunyi Medical University, Zunyi 563000, China.

Email: zh_zmc@foxmail.com

Funding information

National Natural Science Foundation of China, Fund Project Number: 81760079.

Abstract

The main causes of lung injury after cardiopulmonary bypass (CPB) are systemic inflammatory response syndrome (SIRS) and pulmonary ischaemia-reperfusion injury (IR-I). SIRS and IR-I are often initiated by a systemic inflammatory response. The present study investigated whether the annexin A1 (ANX-A1) peptidomimetic Ac2-26 by binding to formyl peptide receptors (FPRs) inhibit inflammatory cytokines and reduce lung injury after CPB. Male rats were randomized to the following five groups (n = 6, each): sham, exposed to pulmonary ischaemic-reperfusion (IR-I), IR-I plus Ac2-26, IR-I plus the FPR antagonist, BoC2 (N-tert-butylloxycarbonyl-Phe-Leu-Phe-Leu-Phe) and IR-I plus Ac2-26 and BoC2. Treatment with Ac2-26 improved the oxygenation index, an effect blocked by BoC2. Histopathological analysis of the lung tissue revealed that the degree of lung injury was significantly less ($P < 0.05$) in the Ac2-26-treated rats compared to the other experimental groups exposed to IR-I. Ac2-26 treatment reduced the levels of the inflammatory cytokines TNF- α , IL-1 β , ICAM-1 and NF- κ B-p65 ($P < 0.05$) compared to the vehicle-treated group exposed to IR-I. In conclusion, the annexin A1 (ANX-A1) peptidomimetic Ac2-26 by binding to formyl peptide receptors inhibit inflammatory cytokines and reduce ischaemic-reperfusion lung injury after cardiopulmonary bypass.

KEYWORDS

Ac2-26, Annexin A1, cardiopulmonary bypass, formyl peptide receptor, ischaemia-reperfusion injury, pulmonary injury

1 | BACKGROUND

Cardiopulmonary bypass (CPB) is a common surgical method used in clinical practice and has been widely used in respiratory cycle support surgery for the heart, large vessel open surgery,

organ transplantation and treatment of several systemic diseases.^{1,2} After the operation, CPB will inevitably result in injury to the internal organs, including post-operative lung injury, which is one of the most common complications and manifests as varying degrees of acute lung injury (ALI) and pulmonary dysfunction, but its mechanism is not yet clear. The most common complications tend to be systemic inflammatory response

Jiyang Xu and Chengkun Yu considered as co-author.

This is an open access article under the terms of the Creative Commons Attribution-NonCommercial-NoDerivs License, which permits use and distribution in any medium, provided the original work is properly cited, the use is non-commercial and no modifications or adaptations are made.

© 2021 The Authors. *Basic & Clinical Pharmacology & Toxicology* published by John Wiley & Sons Ltd on behalf of Nordic Association for the Publication of BCPT (former Nordic Pharmacological Society).

syndrome (SIRS) and ischaemia-reperfusion (IR) injury, in which the systemic inflammatory response induced by various causes is the initiating factor,³ but the specific mechanism is not clear. Studies have shown that a variety of inflammatory cytokines is closely related to CPB lung injury⁴; these important cytokines mainly include tumour necrosis factor α (TNF- α) and interleukin-1 β (IL-1 β).⁵ TNF- α is mainly produced by alveolar mononuclear macrophages, synergistically activates nuclear factor- κ B (NF- κ B) to produce cytokines, induces the aggregation of neutrophils (polymorphonuclear leucocyte, PMN), initiates the early inflammatory response and maintains inflammation⁶ and plays an important role in the occurrence and development of ALI and in the acute respiratory distress syndrome (ARDS) inflammatory response.⁷ Studies have shown that patients with severe lung injury after surgery can develop ARDS, with a mortality rate as high as 30%-50%.^{8,9} Therefore, the study of CPB lung injury mechanisms and lung protection measures has been the main focus of extracorporeal circulation research.

Annexin A1 (ANX-A1) is a 37 kDa endogenous anti-inflammatory protein widely distributed in adult mammals.¹⁰ It has a calcium ion-binding site, interacts with phospholipid-binding proteins and participates in many cell life activities, such as anti-inflammatory reactions, cell differentiation and proliferation, cell death signal regulation and apoptotic cell phagocytosis. Its active function N-terminal Ac2-26 is embedded in the membrane, and the connexin A1 peptide fragment has the biological activity of annexin A1. Elena Y. Senchenkova et al¹¹ showed that ANX-A1 promotes endogenous catabolism in cerebral IR-I and reduces platelet aggregation and thrombosis by affecting integrin (α IIb β 3) activation. This study reveals the multifaceted role of anti-thrombotic-inflammatory circuits as therapeutic and preventive drugs. Han et al showed that¹² in acute radiation-induced lung injury (RILI), ANX-A1 can inhibit the synthesis and secretion of IL-6 and MPO inflammatory cytokines, suggesting that ANX-A1 may have potential as a therapeutic target. Liu L and other studies have shown¹³ that the use of exogenous Ac2-26 plays an important role in microglia and demonstrates that Ac2-26 is associated with HSPB1 and promotes the binding of HSPB1 to IKK β , which is mediated by molecular chaperones. Autophagy (CMA) degrades TNF- α , thereby reducing expression. The above studies show that both AnxA1 and the peptide Ac2-26 can regulate the body's inflammatory response.

Formyl peptide receptor (FPR)¹⁴ is a group of G protein-coupled receptors with seven transmembrane domains that are mainly expressed by mammalian phagocytic leucocytes and play a role in host defence and inflammation. In recent years,¹⁵ ANX-A1 has been found to exert its biological effects by binding to FPR. The study found that^{8,16} the FPR family includes FPR1, FPR2 and FPR3; among them, the FPR2

subtype plays a very important role in the signal transduction of ANX-A1. The initial study found that FPR2/Fpr2 is highly expressed on the surface of neutrophils and monocytes/macrophages, and FPR2/Fpr2 expression was also detected in other immune cells, including basophils, eosinophils, T lymphocytes and B lymphocytes.

As we all know, the formyl peptide receptor (FPR) is the receptor of Ac2-26 and Annexin A1, while Boc2 is the blocker of FPR. Studies have shown that the use of FPR inhibitor Boc-FLFLF inhibits the triggering of the PDR vitreous neovascularization and inflammation.¹⁷ Higher numbers of CXCR4⁺ neutrophils were detected in the circulation of AnxA1-/- or Boc2-treated WT mice, and values were rescued in Ac2-26-treated AnxA1-/- mice. Deletion of AnxA1 reduces the level of CXCL12 in the bone marrow, and Boc2 treatment also produced a similar effect, which reduced the secretion of CXCL12 in WT mice.¹⁸

In summary, ANX-A1 is an important regulator of the endogenous inflammatory response, and FPR2 acts as an important anti-inflammatory receptor for ANX-A1. The combination of the two has an important influence on the development of inflammation.

Our goal through this experiment is to prove that the peptidomimetic Ac2-26 has the effect of reducing lung injury after cardiopulmonary bypass. This research will help find new anti-inflammatory drugs for clinical lung injury after cardiopulmonary bypass. Our experiments demonstrated that the application of the exogenous ANX-A1 peptidomimetic Ac2-26 can reduce lung injury after CPB in rats, reduce the levels of TNF- α , IL-1 β , ICAM-1 and NF- κ B p65 in lung tissue and have a lung protective effect.

The study was conducted in accordance with the Basic & Clinical Pharmacology & Toxicology policy for experimental and clinical studies.¹⁹

2 | EXPERIMENTAL ANIMALS AND METHODS

2.1 | Experimental animals and groupings

A total of 30 male SD rats weighing 350-450g (Changsha Tianqin Biotechnology Co., Ltd, LICENSE number: SCXK(Xiang)2014-0011) were randomly divided into 5 groups of 6 (n = 6): sham operation group (S group), ischaemia-reperfusion injury group (IR-I group), Ac2-26 group (A group), Boc2 group (B group) and Ac2-26 + Boc2 group (AB group). Except for the S group, the other 4 groups had their chests opened 10 minutes after the establishment of CPB, the left hilar was blocked, and lung IR-I in rats was simulated.

2.1.1 | S group

After vascular catheterization, only mechanical ventilation was performed, and the mice did not receive any other treatment.

2.1.2 | IR-I group

A model of CPB IR-I in the left lung was established, and an equal volume of normal saline was injected 10 minutes before the left hilar block.

2.1.3 | A group

A model of left lung CPB IR-I was established, and 1 mg kg⁻¹ Ac2-26 (Tocris Bioscience, Cat. No. 1845) was administered through the tail vein 10 minutes before the left hilar was blocked.

2.1.4 | B group

To establish a model of left lung CPB IR-I, 50 µg of BoC2(N-tert-butyloxycarbonyl-Phe-Leu-Phe-Leu-Phe, Genscript Biotech, Cat. No. RP12950) was administered through the tail vein 10 minutes before left hilar occlusion.

2.1.5 | AB group

To establish a model of left lung CPB IR-I, 50 µg of Boc2 was administered through the tail vein 10 minutes before left hilar occlusion, and 1 mg kg⁻¹ of Ac2-26 was administered simultaneously.

2.2 | Materials

Ac2-26 (Tocris Bioscience, UK. Cat. No. 1845)

BoC2 (N-tert-butyloxycarbonyl-Phe-Leu-Phe-Leu-Phe, Genscript Biotech, Cat. No. RP12950)

Annexin A1 Antibody (Novus Biologicals, Cat. No. NBP2-23485)

Phospho-NF kappaB p65 (Ser536) Antibody (Affinity Biosciences, Cat. No. AF2006)

Rat ICAM-1/CD54 Affinity Purified Polyclonal Antibody (R&D Systems, Cat. No. AF583)

Rat IL-1β ELISA KIT (SHANGHAI WESTANG BIOTECH, China. Cat. No. F15810)

Rat TNF-α ELISA KIT (SHANGHAI WESTANG BIOTECH, Cat. No. F16960)

GEM Premier 3000 system (Werfen company)

2.3 | Preparation of the CPB pipeline

Cardiopulmonary bypass tubing consists of a blood reservoir (20 mL syringe), silicone tubing, peristaltic pump, arteriovenous tubing and rat lung membranes. Before the animal experiment, the CPB pipeline was connected, oxygen was connected, and the CPB pipeline was pre-filled with 1 mL of sodium potassium magnesium calcium glucose injection, 9 mL of hydroxyethyl starch, 1 mL of 5% sodium bicarbonate and 1 mL of mannitol.

2.4 | Establishment of a model of CPB ischaemia-reperfusion injury in the left lung of rats

This experimental model establishes a model of extracorporeal circulation ischaemia-reperfusion injury using He Miao et al.²⁰ Rat anaesthesia was injected intraperitoneally with 1% sodium pentobarbital 50 mg kg⁻¹. After sufficient anaesthesia was administered, the tail vein was placed in the catheter, and the rats were placed in a fixed supine position. The right femoral artery and the left femoral vein were separated, and the catheter was inserted; the trachea was intubated by visualization with a laryngoscope, and the right common carotid artery was punctured and placed. The tracheal tube was connected to a small animal ventilator for mechanical ventilation, maintaining a respiratory rate of 60 times·min⁻¹, a tidal volume of 15 mL kg⁻¹, I:E = 1:2.5 and FiO₂: 99%. The right femoral artery was connected to a biosignal acquisition and processing system to monitor the vital signs, including heart rate and blood pressure. The tail vein was injected with 5 mg kg⁻¹ heparin. After systemic heparinization, the bilateral femoral veins were used for venous drainage, the right common carotid artery was refluxed at the arterial end, and the CPB pipeline was connected. After ACT ≥ 480 seconds, the transfer was started. After 10 minutes, the left lung was closed with a non-invasive vascular clamp, and single-lung ventilation was performed for the right lung. The tidal volume and respiratory rate were appropriately reduced to meet the needs of the body. After 45 minutes of parallel circulation, the non-invasive vascular forceps were released, and the left lung was released. The door restored lung ventilation, increased the tidal volume and reduced the respiratory rate; CPB was stopped after 30 minutes; and the experiment ended after 90 minutes. During the CPB period, the anal temperature was maintained at 32-34°C, the mean arterial pressure was maintained at 50-80 mm Hg, and the perfusion flow rate was 40 ml kg⁻¹ min⁻¹. Before the experiment ended, protamine was injected into the tail vein to neutralize excess heparin. The neutralized machine blood was recovered and input into the rat from the tail vein. Intraoperative arterial blood gas analysis was used to stabilize the rat internal environment using

Pathological changes in lung pathological status

Structural damage	0	Pulmonary blood vessels, interstitial, alveolar and bronchial normal
	1	Interstitial and alveolar haemorrhage oedema range <25%
	2	Interstitial widening, alveolar haemorrhage oedema range 25%-50%
	3	Interstitial significantly widened, alveolar haemorrhage oedema range 50%-75%
	4	Interstitial significantly widened, alveolar haemorrhage oedema range >75%
Inflammation	0	None
	1	Interstitial small amount of neutrophils
	2	Interstitial and some alveolar spaces have more neutrophils
	3	Neutrophils and agglomerates in most of the alveolar spaces

TABLE 1 Pathological scores of lung tissue damage

fentanyl, midazolam and pentobarbital sodium, to maintain the depth of anaesthesia with vecuronium and (if necessary) to maintain the rat vital signs with the use of vasoactive drugs. During the operation, a stomach tube was inserted into the rats for gastrointestinal decompression, and an indwelling catheter was used for intraoperative urine drainage.

2.5 | Specimen collection

A total of 0.5 mL of femoral artery blood from each group were taken before CPB (T1), open left hilar occlusion (T2) and end of experiment (T3), and the intact left lung tissue was cut at the end of the experiment. Blood gas analysis of arterial blood and calculation of the oxygenation index (OI) and respiratory index (RI) were performed. The left lung of the rats was divided into two parts (the upper and lower parts); the upper part of the left lung was examined by light microscopy and electron microscopy; the left part of the left lung was frozen at -80°C , and the expression of TNF- α and IL-1 β in lung tissue was detected by enzyme-linked immunosorbent assay (ELISA). Western blotting was used to detect the expression of AnxA1, p-NF- κB p65 and ICAM-1 in the lung tissue.

2.6 | Indicator detection

2.6.1 | Pulmonary function measurement

OI and RI were calculated based on the results of arterial blood gas analysis.

$$\text{OI} = \text{PaO}_2 / \text{FiO}_2 \quad \text{RI} = \text{P(A-a)O}_2 / \text{PaO}_2$$

$$\text{Remarks: Corrected OI} = \text{PaO}_2 / [\text{FiO}_2 \times (\text{P}/760)]$$

P(A-a)O_2 (alveolar-arterial oxygen partial pressure difference) = $(\text{P} - \text{P}_{\text{H}_2\text{O}}) \times \text{FiO}_2 - \text{PaO}_2 - \text{PaCO}_2 / 0.8$;

PH_2O is the saturated water vapour pressure, which is 47 mm Hg under standard conditions;

P is the actual atmospheric pressure, and the Zunyi area is 680 mm Hg;

FiO_2 (%) is the concentration of inhaled oxygen, and the experimental model of this animal is 99%.

2.6.2 | Light microscopy and pathological damage score of lung tissue

The left lung tissue was fixed with 4% paraformaldehyde and then embedded in paraffin. The paraffin-embedded lung tissues were cut into 3-5 μm slices by a microtome, dehydrated twice in 50% ethanol and n-butanol, dewaxed three times in xylene, HE stained and sealed; the tissue morphology was observed under a light microscope. In addition, pictures were taken.

For the pathology scores, three high-power fields (100 \times) were randomly selected from each pathological section and scored using the method by Cheng C et al.²¹ According to the alveolar and alveolar interstitial areas with noxious swelling, red blood cell exudation and inflammatory cell infiltration, the average was taken as the score of this section (Table 1).

2.6.3 | Lung tissue electron microscopy

The lung tissue was fixed with 2.5% glutaraldehyde at 4°C overnight. The samples were rinsed in PBS, fixed with 1% osmium tetroxide for 1 hour at room temperature, embedded in 10% gelatin, fixed in glutaraldehyde for one hour at 4°C and dehydrated with increasing concentrations of ethanol (30%, 50%, 70%, 90%, 95%, 100%, 100%, 100%). After embedding with epoxy

TABLE 2 Comparison of the Oxygenation Index at different time-points in each group of rats ($n = 6, \bar{x} \pm s$)

Group	T1	T2	T3
S	363.56 ± 19.46	350.41 ± 45.27	334.17 ± 19.10
IR-I	361.93 ± 32.92	195.66 ± 51.71*	126.55 ± 37.40* [#]
A	373.45 ± 25.31	281.16 ± 21.97*	248.67 ± 29.58*
B	366.51 ± 20.05	193.59 ± 30.68*	129.95 ± 35.42* [#]
AB	371.68 ± 18.07	209.69 ± 34.01*	132.16 ± 37.96* [#]

Note:: Compared with T1, * $P < 0.05$; compared with T2, [#] $P < 0.05$. compared with IR-I group, ^a $P < 0.05$.

resin, the tissues were sliced with a Leica UC6 ultramicrotome. Finally, the samples were observed with a transmission electron microscope at 110 kV, and photographs were taken.

2.6.4 | ELISA

The frozen lung tissue was thawed in a refrigerator at 4°C, and the specimen was maintained at a temperature of 2–8°C after thawing. PBS (pH 7.4) was added to the sample, and the specimen was thoroughly ground until homogenized. An ELISA was used to calculate the standard curve using the standard concentration as the abscissa, the OD value as the ordinate and the TNF- α (Rat TNF- α ELISA KIT (SHANGHAI WESTANG BIO-TECH, Cat. No. F16960) and IL-1 β (Rat IL-1 β ELISA KIT, SHANGHAI WESTANG BIO-TECH, Cat. No. F15810) concentrations as the test samples.

2.6.5 | Western blot

Immediately after the experiment, lung tissue was excised and frozen at –80°C. The samples were then centrifuged in ice-cold lysis buffer at 12 000 g for 5 minutes at 4°C. The supernatant (total protein) was collected and stored at –80°C to detect the expression of ANX-A1 (Annexin A1 Antibody, 1:1000, Novus Biologicals, Cat. No. NBP2-23485), p-NF- κ B p65 (Phospho-NF kappaB p65 (Ser536) Antibody, 1:1000, Affinity Biosciences, Cat. No. AF2006), ICAM-1 (Rat ICAM-1/CD54 Affinity Purified Polyclonal Antibody, 0.2 μ g mL⁻¹, R&D Systems, Cat. No. AF583) and GAPDH (Anti-GAPDH antibody [6C5]—Loading Control, 1:1000, Abcam, Cat. No. ab8245). The protein content of the supernatant was determined by a BCA protein assay kit.

2.7 | Statistical methods

The experimental data in this article count the differences in pathology scores, oxygenation index and respiratory index between groups and the expression levels of related proteins and

inflammatory factors. Data analyses and statistical evaluations were carried out using *IBM SPSS* 18.0. All results are the mean standard deviation of at least three experiments performed in triplicate. Data are shown as mean values \pm standard error of the mean (SEM). Multiple comparison between different groups was analysed by one-way ANOVA or Dunnett's T3 test. Differences were considered statistically significant at a value of $P < 0.05$.

3 | RESULTS

3.1 | Changes in OIs and RIs in rats

3.1.1 | Comparison of the same group at different time-points

There was no significant difference in OI and RI of rats in S group at each time-point ($P > 0.05$). Compared with the time-point of T1 in the other four groups, OI at T2 and T3 point was significantly down and RI was significantly increased ($P < 0.05$). There was no significant difference in OI and RI between T2 and T3 in group A ($P > 0.05$).

3.1.2 | Simultaneous comparison of each group

At T1 point, there was no significant difference in OI and RI between each group ($P > 0.05$). At T2, compared with S and A groups, OI of IR-I group decreased significantly ($P < 0.05$), and RI was significantly increased ($P < 0.05$). There was no significant difference in OI and RI between the IR-I, B and AB groups ($P > 0.05$). At T3, OI of S and A groups was significantly higher than IR-I group ($P < 0.05$), while RI was the opposite ($P < 0.05$). There was no significant difference in OI and RI in IR-I, B and AB groups ($P > 0.05$) (Tables 2 and 3, Figure 1A,B).

3.2 | Lung tissue light microscopy results and pathological damage score

The lung tissue structure of the S group was clear, and a small amount of alveolar wall rupture and inflammatory

TABLE 3 Changes in Respiratory Index at different time-points in each group of rats ($n = 6$, $\bar{x} \pm s$)

Group	T1	T2	T3
S	0.508 ± 0.089	0.585 ± 0.223 ^a	0.643 ± 0.102 ^a
IR-I	0.522 ± 0.153	1.970 ± 0.736 ^{*a}	3.694 ± 1.404 ^{*#a}
A	0.469 ± 0.102	0.959 ± 0.160 [*]	1.230 ± 0.272 ^a
B	0.497 ± 0.088	1.914 ± 0.557 ^{*a}	3.529 ± 1.288 ^{*#a}
AB	0.473 ± 0.076	1.680 ± 0.463 ^{*a}	3.500 ± 1.407 ^{*#a}

Note: Compared with T1, ^{*} $P < 0.05$; compared with T2, [#] $P < 0.05$; compared with the IR-I group, ^a $P < 0.05$.

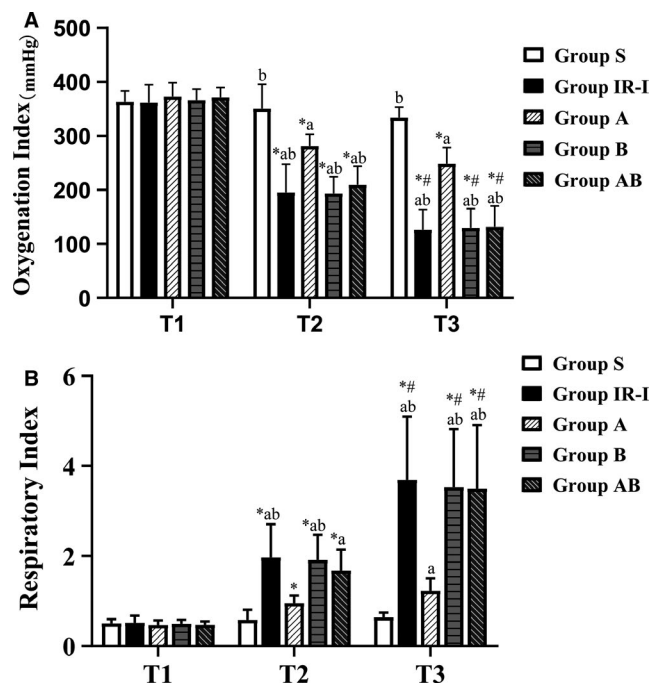


FIGURE 1 Changes in OIs and RIs in rats, A showed the PaO₂/FiO₂ (OI) change in each group at different time. Compared with T1, ^{*} $P < 0.05$; compared with T2, [#] $P < 0.05$. compared with IR-I group, ^a $P < 0.05$. B showed the RI change in each group at different time. Compared with T1, ^{*} $P < 0.05$; compared with T2, [#] $P < 0.05$; compared with the IR-I group, ^a $P < 0.05$

exudation was observed. The lung tissue structure of the A group was clear, some alveolar walls were broken, and a small number of inflammatory cells had infiltrated the tissue. The lung tissue structure of the IR-I, B and AB groups was disordered. The wall was severely broken, the alveolar cavity collapsed and filled with oedema fluid, and a large number of inflammatory cells and red blood cells were infiltrated. Compared with those of the S group, the pathological scores of the lung tissue in group A ($P > 0.05$) and the pathological scores of lung tissue in the IR-I, B and AB groups were not significantly different. There was no significant difference in the pathological scores of lung

tissue from the IR-I group, the B group and the AB group ($P > 0.05$) (Figure 2, Table 4).

3.3 | Lung tissue electron microscopy results

Electron microscopy was used to examine the tissues of the S group, and the structure of the lamellar body was not destroyed, the mitochondria were slightly swollen, and no microvilli appeared in the field of view. Electron microscopy showed that in the IR-I group, the structure of the lamellar body was destroyed, the number of visual fields was reduced, the emptying was increased, the mitochondria were oedematous, and the microvilli structure disappeared. Electron microscopy showed that in the A group, the structure of the lamellar body was mostly intact. The outer layer of the lamellar body was approximately 1 μm in diameter and contained parallel plate-like structures. The mitochondria were slightly oedematous, and the villus structure was faintly visible. In the B group, the lamellar structure was damaged, and the mitochondria were swollen. In the AB group, the lamellar structure was damaged (Figure 3).

3.4 | Expression of ANX-A1 (37 kDa), p-NF- κ B p65 and ICAM-1 in lung tissue at T3

The expression of ANX-A1 (37 kDa) in the lung tissue of the IR-I, B and AB groups was significantly higher than that in the S and A groups ($P < 0.05$). There was no significant difference among expression in the IR-I, B and AB groups ($P > 0.05$) (Table 5, Figure 4A,B).

Compared with the group S, the expression of p-NF- κ B p65 and ICAM-1 in the lung tissues of the IR-I, A, B, AB groups was significantly higher ($P < 0.05$), compared with the A group. In comparison, the expression of p-NF- κ B p65 and ICAM-1 in the lung tissues of the IR-I, B and AB groups was significantly increased ($P < 0.05$); there was no significant difference in the IR-I, B and AB groups ($P > 0.05$; Figure 4A,B).

3.5 | Contents of TNF- α and IL-1 β in lung tissues at T3

There was no significant difference in the expression of TNF- α and IL-1 β in the lung tissues of the IR-I, B and AB groups ($P > 0.05$), but the contents were significantly increased compared with those in the S and A groups ($P < 0.05$). Compared with that in the S group, the TNF- α content was significantly increased in the A group ($P < 0.05$), and IL-1 β was not significantly different ($P > 0.05$); the TNF- α and IL-1 β contents

FIGURE 2 The lung tissue light microscopy results. A is observed S group which was clear, and a small amount of alveolar wall rupture. B is showed IR-I group the alveolar walls were severely broken, the alveolar cavity collapsed and filled with oedema fluid, and a large number of inflammatory cells and red blood cells were infiltrated. C is A group that observed lung tissue structure clear, a small number of inflammatory cells had infiltrated the tissue. D and E are B group and AB group that lung tissue structure was disordered. The alveolar walls were broken and were infiltrated a lots of inflammatory cells and red blood cells. F is the pathological damage score of the lung tissue, compared with S and A groups, ^a $P < 0.05$; compared with IR-I group, * $P < 0.05$

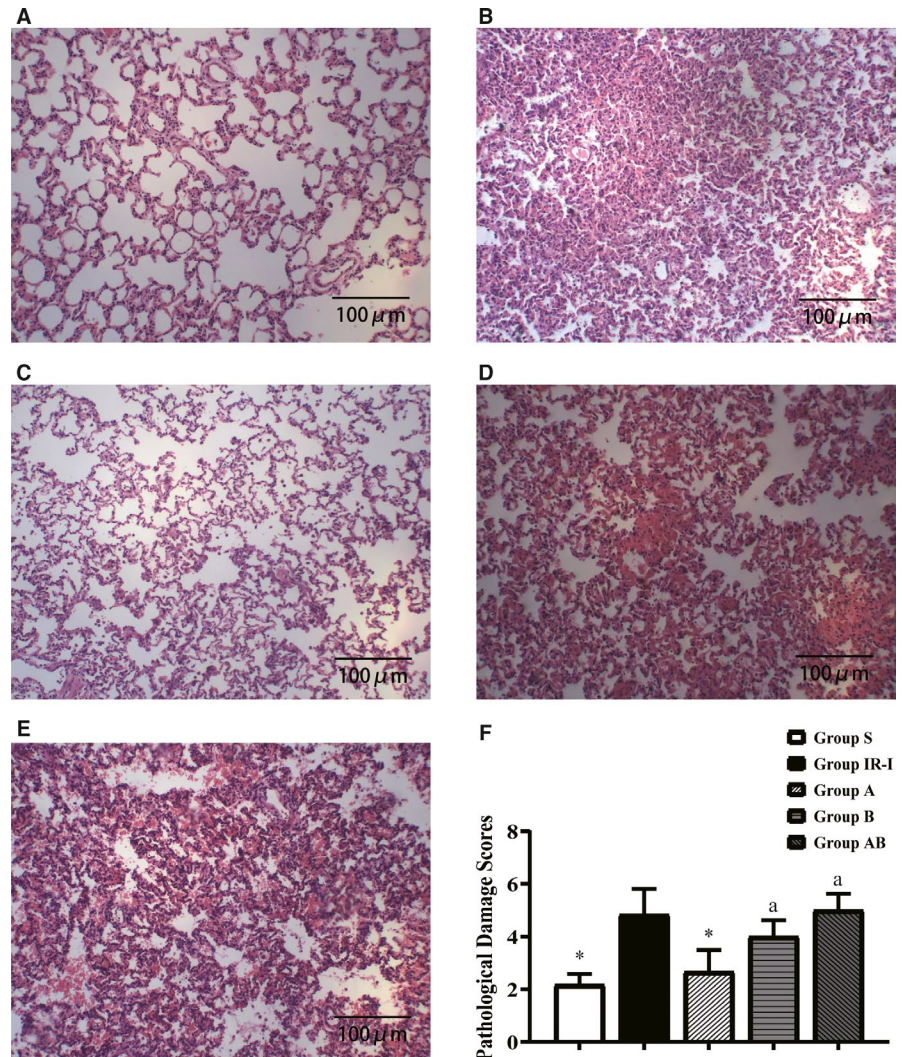


TABLE 4 Pathological damage score of lung tissue in each group of rats at T3

Group	S	IR-I	A	B	AB
Score	2.17 ± 0.41*	4.83 ± 0.98	2.67 ± 0.82*	4.00 ± 0.63 ^a	5.00 ± 0.63 ^a

Note: Compared with the IR-I group, * $P < 0.05$; compared with the IR-I group, ^a $P > 0.05$.

in the A group were significantly lower than those in the IR-I, B, and AB groups ($P < 0.05$) (Table 6, Figure 4C).

4 | DISCUSSION

Acute lung injury is one of the main complications after open heart surgery under CPB.²² The mechanism and prevention measures of CPB lung injury have always been the focus of attention. At present, most scholars believe that the main causes of CPB lung injury are SIRS and lung IR injury, both of which can cause the release of inflammatory cytokines, activate lung endothelial cells and induce the adhesion and infiltration of neutrophils in lung tissue. Studies have shown that²³ during CPB, due to mechanical physics, non-physiological

perfusion, low temperature and other factors, the body's complement system is activated; the complement system activates the immune system response and causes the release of various cytokines,²⁴ such as platelet-activating factor (PAF), interleukin (IL), tumour necrosis factor (TNF) and interferon (IFN)²⁵ to induce the migration and aggregation of neutrophils for pulmonary vascular endothelial cells, alveolar type II epithelial cells, etc Ultimately, this cascade causes damage. Activated neutrophils secrete TNF- α and IL-1 β , which are important substances in the inflammatory response and can act synergistically with other cytokines to promote inflammatory responses by further inducing the release of cytokines and chemokines, and more neutrophils are recruited to the lungs,²⁶ ultimately leading to pulmonary dysfunction during CPB. Studies have shown that TNF- α plays a key role in the

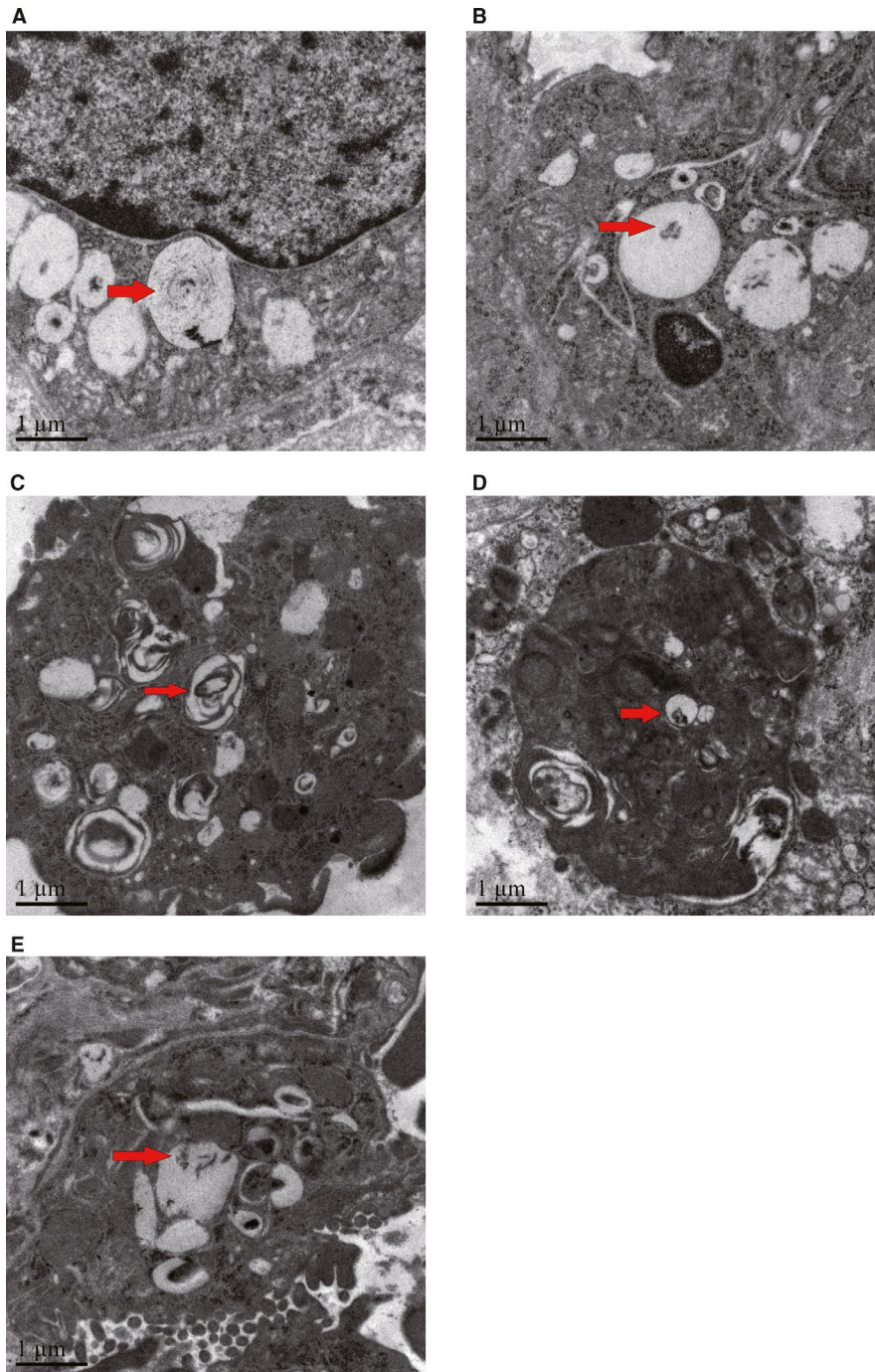


FIGURE 3 Lung tissue electron microscopy. A is S group showing that structure of the lamellar body was not destroyed, and the mitochondria were slightly swollen. B is the IR-I group showing the structure of the lamellar body was destroyed, the number of visual fields was reduced, the emptying was increased, the mitochondria were oedematous, and the microvilli structure disappeared. C is the A group observing that the structure of the lamellar body was mostly intact. D is the B group showing the lamellar structure was damaged, and the mitochondria were swollen. In the AB group, the lamellar structure was damaged just as E shows

TABLE 5 Expression of ANX-A1, p-NF-κB p65 and ICAM-1 in the lung tissues of T3 rats at each time-point

Group	S	IR-I	A	B	AB
AnxA1	0.200 ± 0.04 ^b	0.732 ± 0.06 ^{ac}	0.232 ± 0.03 ^b	0.736 ± 0.05 ^{ac}	0.695 ± 0.07 ^{ac}
p-Nf-κB	0.225 ± 0.02 ^{bc}	0.828 ± 0.06 ^{ac}	0.414 ± 0.04 ^{ab}	0.803 ± 0.07 ^{ac}	0.798 ± 0.07 ^{ac}
ICAM-1	0.243 ± 0.03 ^{bc}	0.967 ± 0.04 ^{ac}	0.404 ± 0.03 ^{ab}	0.986 ± 0.07 ^{ac}	0.951 ± 0.06 ^{ac}

Note: Compared with the S group, ^a*P* < 0.05; compared with the IR-I group, ^b*P* < 0.05, compared with the A group, ^c*P* < 0.05.

pulmonary inflammation caused by CPB. TNF-α can directly induce apoptosis and affect alveolar epithelial cells.²⁷ As an important transcription factor, NF-κB is present in almost all cells, and most of the cytokines related to lung inflammation,

such as TNF-α and ICAM-1, are regulated by NF-κB. Studies have shown that in mice overexpressing NF-κB, LPS-induced pulmonary inflammation is significantly aggravated, leading to more severe pulmonary dysfunction.²⁸ Ac2-26 inhibits

the formation of reactive oxygen species (ROS) induced by TNF- α and reduces the activation of the NF- κ B pathway in endothelial cells.²⁹ Intercellular cell adhesion molecule-1 (ICAM-1) is a transmembrane glycoprotein expressed on the cell surface that is involved in inflammation and immune responses in type I and type II alveolar epithelial cells and pulmonary capillary endothelial cells. Studies have shown that³⁰ ICAM-1 plays an important role in the recruitment of concentrated granulocytes to the lungs. When the ICAM-1 gene is knocked out, TNF- α stimulates vascular permeability and intrapulmonary neutrophils in mice. Cell counts were all

reduced by more than 70%. In the IR injury model induced by limbs in rats, ICAM-1 expression is elevated, and ischaemic post-conditioning can reduce the expression of ICAM-1 and plays a role in lung protection. These studies suggest that systemic inflammatory responses caused by various causes may be the initiating factor of CPB lung injury.³¹ Therefore, how to control the inflammatory response of the whole body or lungs is the key to reducing the lung damage caused by CPB. The study of its mechanism of action may have positive implications for finding new anti-inflammatory drug targets.

The main features of CPB lung injury are impaired lung function and pathological changes in lung tissue. Clinically, RI and OI are commonly used to judge lung function. There is a negative correlation between RI and OI, and changes in either can reflect changes in lung function. Experiments have confirmed that ANX-A1 inhibits the adhesion of PMNs to endothelial cells by inducing L-selectin detachment in neutrophils and simultaneously activates caspase-3 to promote PMN apoptosis to regulate inflammation.³² In a smoke-induced rat lung inflammation model, the use of Ac2-26 alleviated lung epithelial damage caused by smoke exposure.³³ In the IR-induced ALI model, the use of Ac2-26 significantly reduced lung neutrophil infiltration, improved lung injury scores and provided lung protection.³⁴ Studies have shown that under normal conditions, ANX-A1 is mainly inactive in the cytoplasm. Under the action of inflammatory factors, neutrophils bind to capillary endothelial cells, stimulating a large amount of ANX-A1 to move to the cell surface with calcium ions. ANX-A1 is anchored on the serosal membrane of the cell and interacts with adhesion molecules, mediating the interaction between leucocytes and endothelial cells, thereby inhibiting leucocyte migration to the site of inflammation and regulating the body's own anti-inflammatory effects. The expression of ANX-A1 in the lung tissue of rats in the IR group after CPB was significantly higher than that in the S group and A group, but the pathological damage, lung function and systemic condition of the lung tissue were not improved. The reason may be a strong systemic inflammatory response caused by CPB, which stimulates the body to significantly increase AnxA1 expression in the lung tissue. During this process, activated neutrophils release various proteases and cause lung tissue damage. The expression of TNF- α , IL-1 β , p-NF- κ B p65 and ICAM-1 in the lung tissue of the A group was lower than that of the IR group,

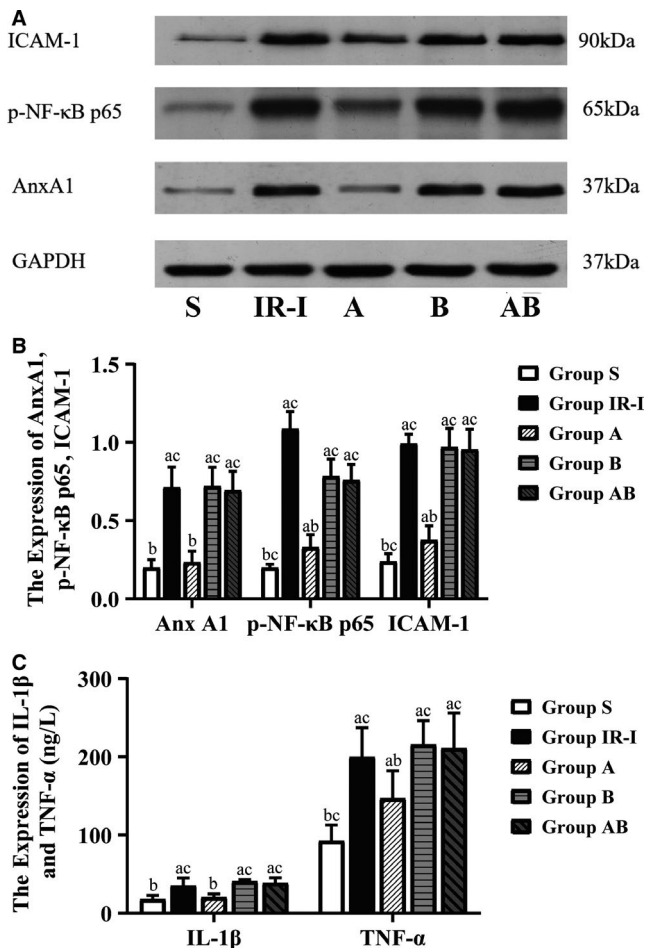


FIGURE 4 Expression of ANX-A1 (37 kDa), p-NF- κ B p65, ICAM-1, TNF- α and IL-1 β . A is the Western Blot strip of ANX-A1, p-NF- κ B p65 and ICAM-1. B is the histogram of ANX-A1, p-NF- κ B p65 and ICAM-1, compared with IR-I group ($P < 0.05$). C is the histogram of TNF- α and IL-1 β , compared with IR-I group ($P < 0.05$)

TABLE 6 Expression of TNF- α and IL-1 β in the lung tissues of rats at each time-point of T3 (ng L⁻¹)

Group	S	IR-I	A	B	AB
IL-1 β	17.9 \pm 4.9 ^b	35.0 \pm 10.0 ^{ac}	20.6 \pm 4.1 ^b	40.9 \pm 2.2 ^{ac}	38.8 \pm 6.5 ^{ac}
TNF- α	92.5 \pm 20.4 ^{bc}	199.9 \pm 37.3 ^{ac}	146.9 \pm 35.3 ^{ab}	215.5 \pm 30.8 ^{ac}	211.0 \pm 45.0 ^{ac}

Note: Compared with the S group, ^a $P < 0.05$; compared with the IR-I group, ^b $P < 0.05$, compared with the A group, ^c $P < 0.05$.

and the degree of lung injury was also less than that of the IR group. However, the expression of AnxA1 (37 kDa) in the lung tissue was significantly lower than that in the IR group. There was no significant difference between the two groups. The reason may be that (a) the inflammation caused by lung IR was inhibited after adding Ac2-26³³; (b) in the COPD model,³⁵ Lucas et al proposed that the reduction in endogenous ANX-A1 after Ac2-26 injection was associated with negative feedback regulation. (c) There are also studies³⁶ indicating that Ac2-26 may regulate the conversion of endogenous ANX-A1 between 37 and 34 kDa. In lung injury caused by distal intestinal ischaemia,³⁷ ANX-A1 expression at 37 kDa was decreased in the lung after Ac2-26 treatment, and ANX-A1 expression at 33 kDa was significantly increased, which was consistent with the results of this experiment and further research.

The specific molecular mechanism of the anti-inflammatory effect of ANX-A1 is not well understood; in recent years,¹⁵ it was discovered that ANX-A1 binds to the FPR to exert its biological function. When an inflammatory response occurs, ANX-A1 binds to FPR, undergoes a series of reactions to inhibit the migration of neutrophils and monocytes and down-regulates the aggregation and adhesion of leucocytes at the site of injury or infection. Perretti found that¹⁶ glucocorticoid-induced ANX-A1 binds to FPR1 and initiates a downstream cascade that promotes extracellular regulated protein kinases (ERKs) and mitogen-activated protein kinases (MAPKs). Phosphorylation affects the activity of the downstream transcription factors AP1 and NF- κ B and cytokines and exerts an anti-inflammatory effect. Endogenous and exogenous ANX-A1 binds to the FPR receptor on the PMN to reduce adhesion and aggregation of the PMN^{38,39}; studies have shown that⁴⁰ Ac2-26 can be reduced in combination with FPR receptors. The interaction of neutrophil-endothelial cells lowers pulmonary arterial pressure, reduces inflammatory cytokine production, reduces lung IR damage and reduces myeloperoxidase activity. Boc2 is an FPR receptor antagonist that binds to FPR1 and FPR2 to block its biological function. After adding Boc2 to the CPB of the experimental rats, it was found that the B, AB and A groups showed a significant decrease in their OIs, a significant increase in their RIs, an increase in the lung pathological scores and damage to the platelet structures of lung tissue under electron microscopy. The expression of TNF- α , IL-1 β and p-NF- κ B p65 in the lung tissue increased significantly. There was no significant difference between the B, AB and IR groups, indicating that Boc2 blocked the AnxA1 peptidomimetic Ac2-26 on rat CPB. The protective effect on the lung tissue suggests that the mechanism of action of Ac2-26 on the lung protection of rat CPB depends on a series of biological effects of the combination of AnxA1 and its receptor FPR.

Although several studies have shown that the binding of annexin A1 to FPRs can effectively reduce the occurrence

and development of endogenous inflammation in vivo, Rahman et al found that⁴¹ FPRs can help the body. The influenza virus is transported into the cell, and the transfection of the virus was significantly reduced after the use of the FPR antagonist WRW4; and Schloer et al⁴² found that the activation of the FPR by annexin A1 can effectively reduce the replication of influenza virus and reduce lung damage.

Therefore, the role and mechanism of annexin A1 and its FPR in the development of endogenous inflammation in vivo require further research to find a new anti-inflammatory therapy.

5 | CONCLUSION

1. The application of the exogenous AnxA1 peptidomimetic Ac2-26 can alleviate lung injury after CPB in rats and reduce the levels of TNF- α , IL-1 β , ICAM-1 and NF- κ B p65 in lung tissue and protect the lungs.
2. The mechanism of the ANX-A1 peptidomimetic Ac2-26 to alleviate lung injury in CPB may be related to the FPR receptor and a reduction in the expression of TNF- α , IL-1 β , ICAM-1 and p-NF- κ B p65 in the rat lung tissue.

CONFLICT OF INTEREST

We declare that we have no financial and personal relationships with other people or organizations that can inappropriately influence our work, there is no professional or other personal interest of any nature or kind in any product, service and/or company that could be construed as influencing the position presented in, or the review of, the manuscript entitled.

AUTHOR CONTRIBUTION

Chengkun Yu designed the experimental project, conducted most of the experiments and prepared the manuscript. Jiyang Xu participated in the establishment of an in vitro lung IR injury model and participated in the writing and revision of the manuscript. Junli Luo and Yuhan Guo completed the analysis of part of the experimental data, and Chi Cheng, as the instructor, completed most of the experimental operation techniques. Hong Zhang revised the paper and had primary responsibility for final content. All authors read and approved the final manuscript.

DATA AVAILABILITY STATEMENT

Data sets used and/or analysed in the current research may be obtained from the authors upon reasonable request.

ORCID

Jiyang Xu  <https://orcid.org/0000-0002-1781-5295>

Hong Zhang  <https://orcid.org/0000-0002-8871-0124>

REFERENCES

- Guay J, Kopp S. Epidural analgesia for adults undergoing cardiopulmonary bypass with or without cardiopulmonary bypass. *Cochrane Database Syst Rev*. 2019;1(3):54-59.
- Michalski M, Pagowska-Klimek I, Thiel S, et al. Factors involved in initiation and regulation of complement lectin pathway influence postoperative outcome after pediatric cardiac surgery involving cardiopulmonary bypass. *Sci Rep*. 2019;9(1):10.
- Durham AL, Al Jaaly E, Fiorentino F, et al. Ischemic lung injury following cardio-pulmonary bypass (cpb) is associated with inflammation and differentiation. C67. ACUTE LUNG INJURY. *Am J Respir Crit Care Med*. 2016;193:A5790.
- Yu Y, Gao M, Li H, Zhang F, Gu C. Pulmonary artery perfusion with anti-tumor necrosis factor alpha antibody reduces cardiopulmonary bypass-induced inflammatory lung injury in a rabbit model. *PLoS One* 2013;8(12):e83236.
- Zhang Z, Wu Y, Zhao Y, Xiao X, Liu J, Zhou X. Dynamic changes in HMGB1 levels correlate with inflammatory responses during cardiopulmonary bypass. *Exp Ther Med*. 2013;5(5):1523-1527.
- Luan ZG, Zhang J, Yin XH, Ma XC, Guo RX. Ethyl pyruvate significantly inhibits tumour necrosis factor- α , interleukin-1 β and high mobility group box 1 releasing and attenuates sodium taurocholate-induced severe acute pancreatitis associated with acute lung injury. *Clin Exp Immunol*. 2013;172(3):417-426.
- Lomas-Neira J, Perl M, Venet F, Chung CS, Ayala A. The role and source of tumor necrosis factor- α in hemorrhage-induced priming for septic lung injury. *Shock*. 2012;37(6):611-620.
- Sugimoto MA, Vago JP, Teixeira MM, et al. Annexin A1 and the resolution of inflammation: modulation of neutrophil recruitment, apoptosis, and clearance. *J Immunol Res*. 2016;2016:1-13.
- Huffmyer JL, Groves DS. Pulmonary complications of cardiopulmonary bypass. *Best Pract Res Clin Anaesthesiol*. 2015;29(2):163-175.
- Buckingham JC, Flower RJ. Chapter 25 – Annexin A1. In: Fink G, ed. *Stress: Neuroendocrinology and Neurobiology*. San Diego, CA: Academic Press; 2017:257-263.
- Senchenkova EY, Ansari J, Becker F, et al. A novel role for the AnxA1-Fpr2/ALX signaling axis as a key regulator of platelet function to promote resolution of inflammation. *Circulation*. 2019;140:319-335.
- Han G, Lu K, Xu W, et al. Annexin A1-mediated inhibition of inflammatory cytokines may facilitate the resolution of inflammation in acute radiation-induced lung injury. *Oncol Lett*. 2019;18(1):321-329.
- Liu L, An D, Xu J, et al. Ac2-26 induces IKK β degradation through chaperone-mediated autophagy via HSPB1 in NCM-treated microglia. *Front Mol Neurosci*. 2018;11:76.
- Ye RD, Boulay F, Wang JM, et al. International Union of Basic and Clinical Pharmacology. LXXIII. Nomenclature for the formyl peptide receptor (FPR) family[J]. *Pharmacol Rev*. 2009;61(2):119-161.
- Spurr L, Nadkarni S, Pederzoli-Ribeil M, et al. Comparative analysis of Annexin A1-formyl peptide receptor 2/ALX expression in human leukocyte subsets. *Int Immunopharmacol*. 2011;11(1):55-66.
- Perretti M, D'Acquisto F. Annexin A1 and glucocorticoids as effectors of the resolution of inflammation. *Nat Rev Immunol*. 2009;9(1):62-70.
- Rezzola S, Corsini M, Chiodelli P, et al. Inflammation and N-formyl peptide receptors mediate the angiogenic activity of human vitreous humour in proliferative diabetic retinopathy. *Diabetologia* 2017;60(4):719-728.
- Machado ID, Spatti M, Hastreiter A, et al. Annexin A1 Is a physiological modulator of neutrophil maturation and recirculation acting on the CXCR4/CXCL12 pathway. *J Cell Physiol*. 2016;231(11):2418-2427.
- Tveden-Nyborg P, Bergmann TK, Jessen N, Simonsen U, Lykkesfeldt J. BCPT policy for experimental and clinical studies. *Basic Clin Pharmacol Toxicol*. 2021;128(1):4-8.20.
- He M, Zhang Y, Xie F, Dou X, Han M, Zhang H. Role of PI3K/Akt/NF- κ B and GSK-3 β pathways in the rat model of cardiopulmonary bypass-related lung injury. *Biomed Pharmacother*. 2018;106:747-754.
- Cheng C, Li SS, Wang Y, et al. Ischemic postconditioning alleviates lung injury and maintains a better expression of aquaporin-1 during cardiopulmonary bypass. *Chin Med J (Engl)*. 2014;127(23):4012-4018.
- Stephens RS, Shah AS, Whitman GJR. Lung injury and acute respiratory distress syndrome after cardiac surgery. *Ann Thorac Surg*. 2013;95(3):1122-1129.
- Cao QF, Qu MJ, Yang WQ, et al. Ischemia postconditioning preventing lung ischemia-reperfusion injury. *Gene* 2015;554(1):120.
- Wen M, Li Z, Zhou L, et al. Protective effects of acupuncture in cardiopulmonary bypass-induced lung injury in rats. *Inflammation* 2017;40(4):1275-1284.
- Peng CK, Oho AUID, Huang KL, et al. Experimental chronic kidney disease attenuates ischemia-reperfusion injury in an ex vivo rat lung model. *PLoS One*. 2017;12(3):e0171736.
- Guma M, Ronacher L, Liu-Bryan R, et al. Caspase 1-independent activation of interleukin-1 β in neutrophil-predominant inflammation. *Arthritis Rheum*. 2009;60(12):3642-3650.
- Gao M, Xie B, Gu C, et al. Targeting the proinflammatory cytokine tumor necrosis factor- α to alleviate cardiopulmonary bypass-induced lung injury. *Mol. Med. Rep*. 2015;11(4):2373-2378.
- Lopez B, Maisonet TM, Londhe VA. Alveolar NF- κ B signaling regulates endotoxin-induced lung inflammation. *Exp. Lung Res*. 2015;41(2):103-114.
- Peshavariya HM, Taylor CJ, Goh C, et al. Annexin peptide Ac2-26 suppresses TNF α -induced inflammatory responses via inhibition of Rac1-dependent NADPH oxidase in human endothelial cells. *PLoS One* 2013;8(4):e60790.
- He B, Geng S, Zhou W, et al. MMI-0100 ameliorates lung inflammation in a mouse model of acute respiratory distress syndrome by reducing endothelial expression of ICAM-1. *Drug Des Devel Ther*. 2018;12:4253.
- Kasper B, Salameh A, Krausch M, et al. Epigallocatechin gallate attenuates cardiopulmonary bypass-associated lung injury. *J Surg Res*. 2016;201(2):313-325.
- Kasikara C, Doran AC, Cai B, et al. The role of non-resolving inflammation in atherosclerosis. *J Clin Invest*. 2018;128(7):2713-2723.
- Possebon L, Costa SS, Souza HR, et al. Mimetic peptide AC2-26 of annexin A1 as a potential therapeutic agent to treat COPD. *Int Immunopharmacol*. 2018;63:270-281.
- Liao WI, Wu SY, Wu GC, et al. Ac2-26, an annexin A1 peptide, attenuates ischemia-reperfusion-induced acute lung injury. *Int J Mol Sci*. 2017;18(8):1771.
- Lucas P, Costa SS, Souza HR, et al. Mimetic peptide AC2-26 of annexin A1 as a potential therapeutic agent to treat COPD. *Int Immunopharmacol*. 2018;63:270-281.

36. La M, D'Amico M, Bandiera S, et al. Annexin I peptides protect against experimental myocardial ischemia-reperfusion: analysis of their mechanism of action. *FASEB J*. 2001;15(12):2247.
37. Guido BC, Zanatelli M, Tavares-de-Lima W, et al. Annexin-A1 peptide down-regulates the leukocyte recruitment and up-regulates interleukin-10 release into lung after intestinal ischemia-reperfusion in mice. *J Inflamm (Lond)*. 2013;10(1):10.
38. Moraes LA, Ampomah PB, Lim LHK. Annexin A1 in inflammation and breast cancer: a new axis in the tumor microenvironment. *Cell Adh Migr*. 2018;12(5):417-423.
39. Hughes EL, Becker F, Flower RJ, et al. Mast cells mediate early neutrophil recruitment and exhibit anti-inflammatory properties via the formyl peptide receptor 2/lipoxin A4 receptor. *Br J Pharmacol*. 2017;174(14):2393-2408.
40. Qin C, Yang YH, May L, et al. Cardioprotective potential of annexin-A1 mimetics in myocardial infarction. *Pharmacol Ther*. 2015;148:47-65.
41. Rahman F, Chebbo M, Courtin N, Fotso Fotso A, Alessi MC, Riteau B. The annexin A1 receptor FPR2 regulates the endosomal export of influenza virus. *Int J Mol Sci*. 2018;19(5):1400
42. Schloer S, Hubel N, Masemann D, et al. The annexin A1/FPR2 signaling axis expands alveolar macrophages, limits viral replication, and attenuates pathogenesis in the murine influenza A virus infection model. *FASEB J*. 2019;33:12188-12199.

How to cite this article: Xu J, Yu C, Luo J, Guo Y, Cheng C, Zhang H. The role and mechanism of the annexin A1 peptide Ac2-26 in rats with cardiopulmonary bypass lung injury. *Basic Clin Pharmacol Toxicol*. 2021;128:719–730. <https://doi.org/10.1111/bcpt.13561>